Infacon XV: International Ferro-Alloys Congress, Edited by R.T. Jones, P. den Hoed, & M.W. Erwee,
Southern African Institute of Mining and Metallurgy, Cape Town, 25–28 February 2018

Mechanism and kinetic modelling of methane-based reduction of Mamatwan manganese ore

A. Bhalla and R.H. Eric
University of the Witwatersrand, Johannesburg, South Africa

Abstract – Reduction behaviour of South African Mamatwan manganese ore using a methane-argon-hydrogen gas mixture was investigated experimentally in the temperature range of 1050°C to 1250°C. The effects of changing gas mixture composition, time, and temperature were studied. It was observed that the bulk of the metallization occurred in the first thirty minutes, and the maximum total metallization reached 73% at 1200°C. The extent of reduction and the Mn/Fe ratios in the resulting alloy were significantly higher than those seen in carbothermic solid-state reduction at similar temperatures, due to lower oxygen potential set up by the very high activity of carbon of the methane-bearing gas mixtures. It was seen that metallization of Mamatwan ore proceeded in two stages. First, reduction of the higher oxides to MnO. Second, reduction of MnO and FeO to mixed carbide of iron and manganese. Mathematical modelling of the kinetics of the process yielded, for the first stage, effective diffusivities for CO/CO_2 lying in the range from 1.45×10^{-6} to $8.427 \times 10^{-6} cm^2 s^{-1}$ at 1100°C. The apparent activation energy for the first stage, in the temperature range of 1050°C to 1250°C, varied from 1.464 kJ/mol to 24.72 kJ/mol which was very low. The rate of metallization during the second stage changed between $1.83 \times 10^{-8} mol.s^{-1}.cm^{-2}$ and $8.55 \times 10^{-8} mol.s^{-1}.cm^{-2}$. The specific rate constant values for the second stage (ks), varied from 5.53×10^{-6} cm/s to 3.16×10^{-5} cm/s, which are smaller than the specific rate constant for the first stage of reduction (kf), which varied from 1.64×10^{-4} cm/s to 1.146×10^{-4} cm/s, as the rate of the second stage is much slower than the rate of the first stage. Mathematical modelling of the kinetics indicated that the chemical reaction was not the likely rate control mechanism for the first stage. Diffusional control seemed to dominate the first stage. The slow second-stage rate control appeared to be mixed, involving both chemical reaction rate and diffusion rate. X-ray analysis revealed that manganese ore was reduced primarily to carbide Mn_7C_3 at the lower temperature range of the experiments, but, at 1200°C, the dominant reaction product was Mn_5C_2. The SEM images showed the product metallic phase occurring throughout the surface, with globular formation in the case of a reduction reaction where hydrogen was the carrier gas.

Keywords: manganese, Mamatwan, reduction, kinetic, modelling

INTRODUCTION

South Africa is the largest producer of manganese ore, followed by Australia. The most significant manganese ore deposits in South Africa are located in the Northern Cape province. A gap of 55 km separates them into the southern field and northern field, which are continuous from the Mamatwan mine in the south to the Wessels mine in the north. The Mamatwan ore is composed chiefly of braunite, with a smaller amount of manganite, hausmannite, and hematite (Burucu, 1991). For the production of ferromanganese and manganese metal, South African high-grade manganese ores, such as those from the Wessels and Hotazel deposits, have been used, but with time they are becoming depleted. It is, therefore, important that the large reserves of medium-grade manganese ore, such as Mamatwan ore, be utilized to a larger extent, even if this requires alternative techniques. The degree and mechanism of the reduction of Mamatwan manganese ore with graphite was studied at laboratory scale by Grimsley (1977). A study (Ostrovski & Zang, 2006) done on reduction of manganese ores using CH_4-H_2-Ar gas mixture found that the high extent and rate of

reduction by methane-containing gas, in comparison with carbothermic reduction, were attributed to high carbon activity in the reducing gas.

Electric smelting and blast furnace processes are used for the production of manganese ferro-alloys by carbothermic reduction of manganese oxides. The electrical furnace has many advantages, such as high yield of Mn from the ore, lower carbon consumption, lower required quality of reducing agents, and greater flexibility in providing different grades of alloys. Electrical furnaces can be used for the production of both HCFeMn (energy consumption around 2400–2800 kWh/t) and SiMn (energy consumption around 3500–4500 kWh/t); therefore, they provide more flexibility according to requirements. Blast furnace smelting has serious disadvantages, such as high coke consumption and loss of manganese in slag.

EXPERIMENTAL

South African Mamatwan ore was used for this study. The composition of the ore is presented in Table I. The manganese particle size class of -150 μm +106 μm was chosen for all the reduction tests.

Table I: Chemical composition of Mamatwan manganese ore

Component	(Mass %)
Mn	37.69
Fe	4.71
SiO_2	4.51
CaO	16.51
MgO	3.29
Al_2O_3	0.231
P	0.0174

The reduction experiments were carried out in a molybdenum wound furnace surrounding a thermo gravimetric (TGA) system from the bottom. Experimental details were similar to ones discussed elsewhere (Akdogan, 1992; Burucu, 1991). The reduction behaviour of manganese particles exposed to methane/hydrogen- and methane/argon-containing gas was assessed on the percent metallization results for the reducible components Mn and Fe. The ore was first calcined at a temperature around 1000°C to drive off the CO_2, as it contained carbonates, then tests were carried out. Reduction tests were run for 10, 20, 30, 60, 90, and 120 minutes. The experimental variables were time, concentration of methane in argon, and concentration of methane in hydrogen gases, and temperature. After each test, a sample was split into three portions; one was taken for wet chemical analysis for metallization values. The degree of metallization was calculated using the following equations:

$$Met._{Mn} = (Mn^0 / Mn_{Total}) \quad [1]$$

$$Met._{Fe} = (Fe^0 / Fe_{Total}) \quad [2]$$

$$Met._{Total} = (Mn^0 + Fe^0) / (Mn_{Total} + Fe_{Total}) \quad [3]$$

where Mn_{Total} and Fe_{Total} represent total Mn and Fe in the product expressed as a percentage of the total product mass; Mn^0 and Fe^0 represent metallized Mn and Fe in the product expressed as percentage of the total product mass; and $Met._{Mn}$, $Met._{Fe}$, $Met._{Total}$ represent manganese, iron, and total metallization respectively.

The other two portions were prepared for scanning electron microscopy (SEM) and X-ray diffraction (XRD). The effect of the hydrogen as the reductant was investigated by running tests at 1100°C and 1200°C using 100% (v/v) H_2 (flow rate: 880 ml/min) on the 2 gram manganese ore sample. The loss of mass was measured using the TGA system (Akdogan, 1992; Burucu, 1991). It was observed that reduction occurred in H_2 with a maximum loss of mass within the first 30–40 minutes. The effect of relative concentration of methane in argon/methane and in hydrogen/methane gas mixtures on the metallization/reduction behaviour of the manganese ore particle was measured in two separate test series. The concentration of methane in both gas mixtures was changed from 10% to 20% and then to 30% (all volume percentages) at a total flow rate of 880 ml/min. The experiments were conducted at temperatures of 1050°C, 1100°C, 1200°C, and 1250°C.

RESULTS AND DISCUSSION

The most significant factor influencing the reduction/metallization rate and degree, as well as kinetic calculations, for methane in argon runs (Anacleto *et al.*, 2004; Kononov *et al.*, 2008; Pomfret & Grieveson, 1978) was temperature. Around a threefold increase was observed in metallization extent from 1050°C to 1250°C (with 10% methane in argon and 30% methane in argon), as illustrated in Figures 1 and 2.

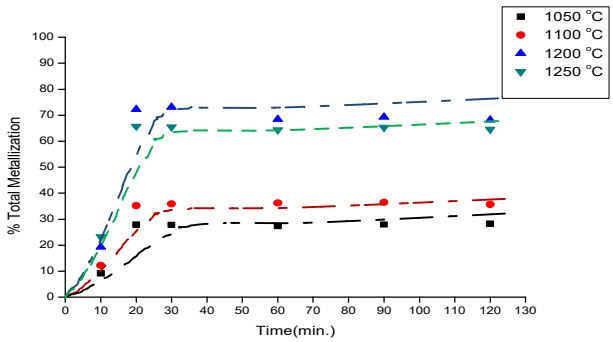

Figure 1: Total metallization for 10% CH_4 in Ar at different temperatures

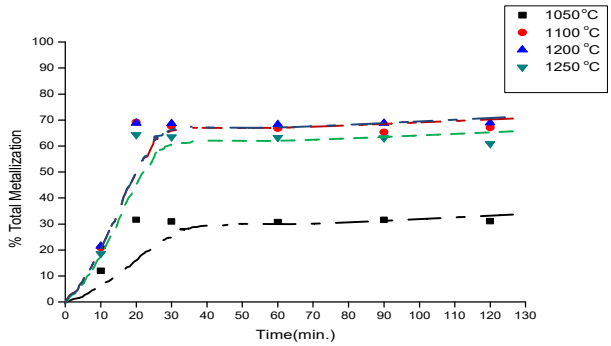

Figure 2: Total metallization for 30% CH_4 in Ar at different temperatures

In the case of runs using methane in hydrogen, such increases with temperature were not observed, as shown in Figures 3 and 4. This may potentially be attributed to constant activity of carbon particles in the methane-hydrogen gas mixtures at a fixed

temperature, which may be lower than in methane-argon gas mixtures at the same temperature.

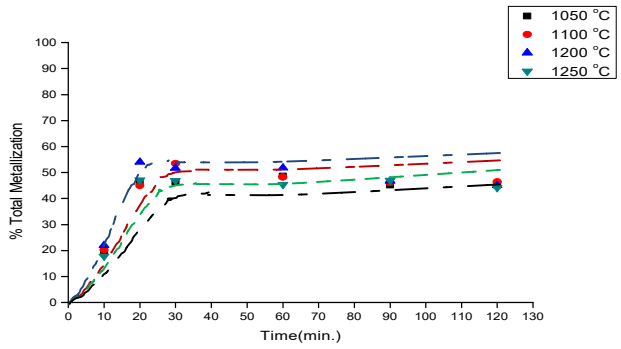

Figure 3: Total metallization for 10% CH_4 in H_2 at different temperatures

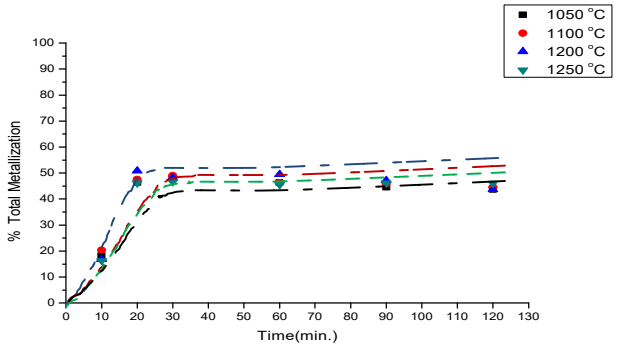

Figure 4: Total metallization for 30% CH_4 in H_2 at different temperatures

Effect of changing argon and hydrogen concentration

The initial rate of reduction was higher for 10% CH_4 in H_2 than for the 10% CH_4 in Ar. For the 30% CH_4 concentration in the two carrier gases at the highest reduction temperature of 1250°C, the highest metallization levels were seen with 30% CH_4 in Ar having a higher metallization extent. This is followed in magnitude by the two metallization curves at 1200°C, which also had a difference between metallization values for the two carrier gases; again with 30% CH_4 in Ar having a higher metallization value. The lowest metallization rate and progress of metallization occurred at 1100°C with hydrogen as the carrier gas. The kinetic difference between 10% to 30% CH_4 in H_2 emphasized the specific importance and significant role of CH_4 in the system. Figures 6 to 13 at the end of this section summarise the metallization results.

A general observation showed that more carbon was present in the samples reduced by CH_4 in H_2 carrier gas. 30% CH_4 in H_2 contained the most total carbon. Figure 5 shows the total metallization value at different temperatures for different mixtures of gases.

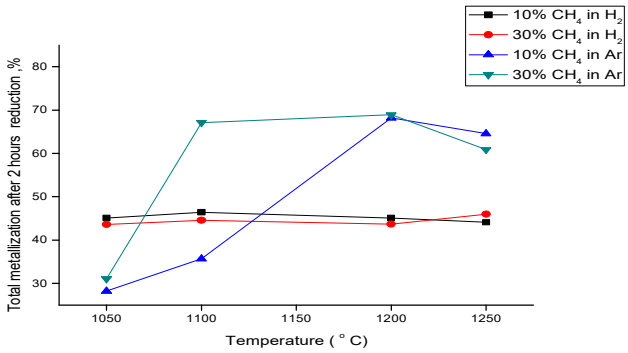

Figure 5: Total metallization as a function of temperature for 2 hours of reduction time

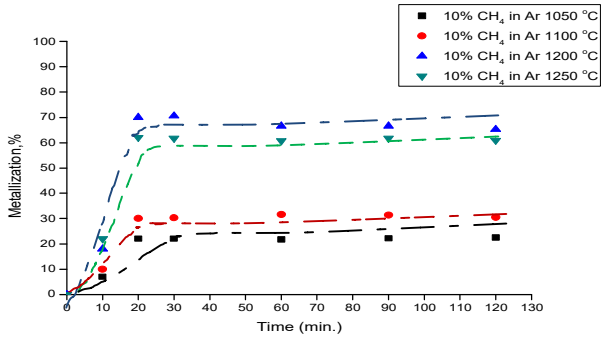

Figure 6: Mn metallization in 10% CH_4 in Ar as a function of time and temperature

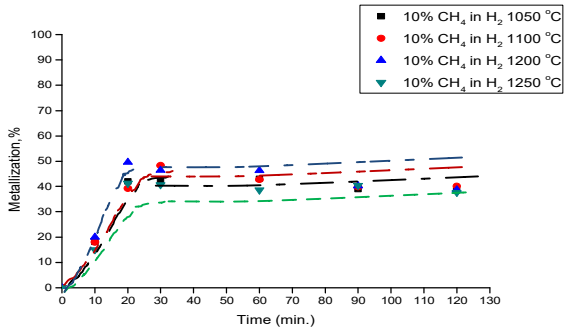

Figure 7: Mn metallization in 10% CH_4 in H_2 as a function of time and temperature

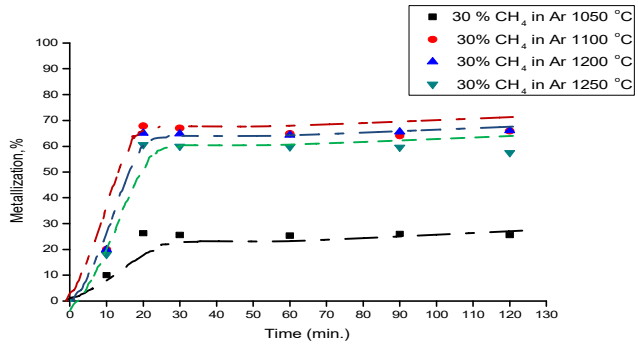

Figure 8: Mn metallization in 30% CH_4 in Ar as a function of time and temperature

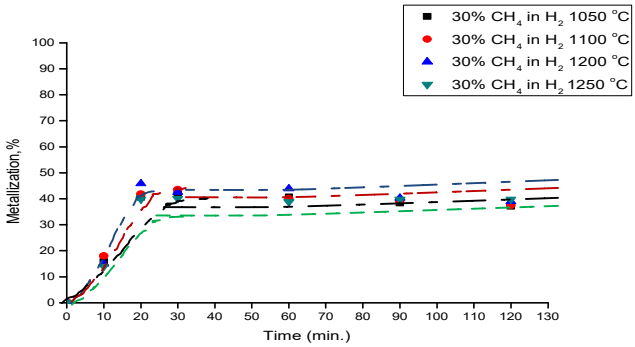

Figure 9: Mn metallization in 30% CH_4 in H_2 as a function of time and temperature

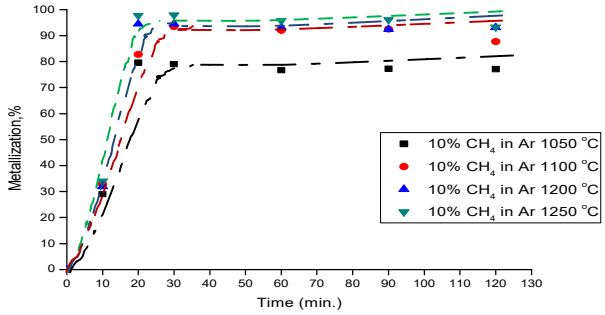

Figure 10: Fe metallization in 10% CH_4 in Ar as a function of time and temperature

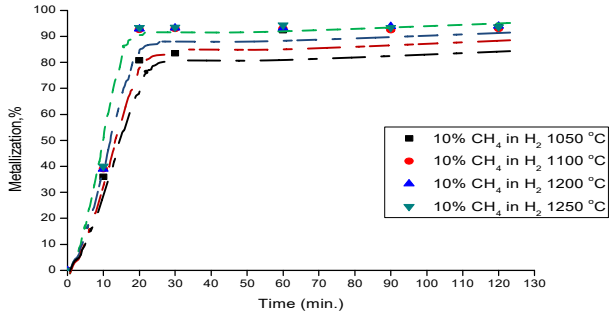

Figure 11: Fe metallization in 10% CH_4 in H_2 as a function of time and temperature

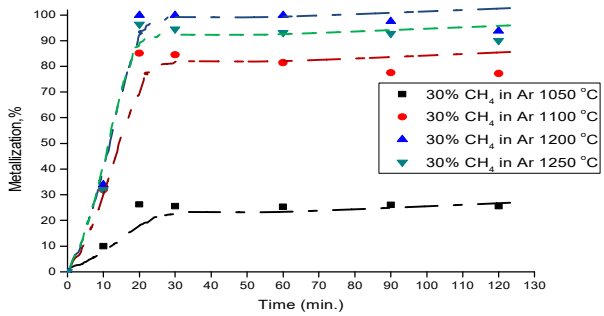

Figure 12: Fe metallization in 30% CH_4 in Ar as a function of time and temperature

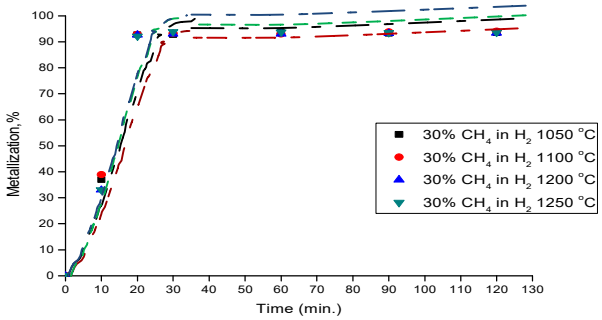

Figure 13: Fe metallization in 30% CH_4 in H_2 as a function of time and temperature

Effect of changing Mn/Fe ratio

Comparing the Mn/Fe metallization curves showed that the Fe and Mn curves as a function of time were approximately linear with time, as shown in Figures 14 and 15. It also showed that the results of 10% CH_4 in Ar have the steepest curve, indicating that the Mn component gradually increased in metallization over time, relative to Fe. For the other gas mixtures, the profiles were rather flat, indicating simultaneous rates for reduction of the Fe and Mn, after the original burst of metallization that occurred in the first 30 minutes. The hydrogen carrier gases had higher Mn/Fe metallization ratios, due to the more rapid reduction rate that occurred in the first 30 minutes.

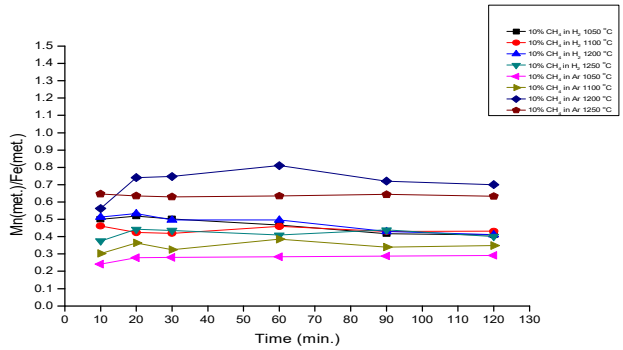

Figure 14: Mn/Fe metallization ratios at 10% CH_4 concentrations in H_2 and Ar

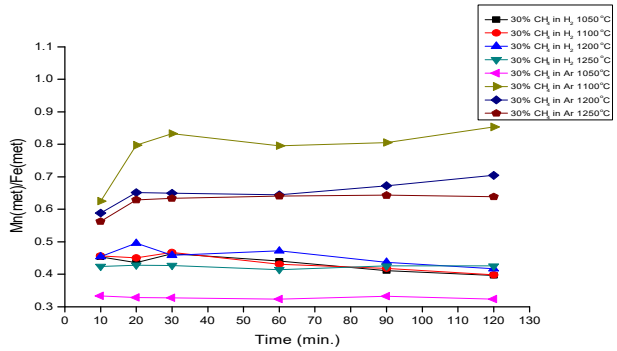

Figure 15: Mn/Fe metallization ratios at 30% concentrations in H_2 and Ar

The Reduction Mechanism

For this study, a mathematical model was developed. It was seen that metallization of Mamatwan ore proceeded in two stages, as was deduced from an examination of the partially reduced / metallized samples.

Stage 1: The reduction of the higher oxides to MnO, metallization of iron, and start of metallization of manganese.

Stage 2: After about 30 minutes, the kinetically slow and long stage 2 starts, during which partial reduction of MnO and any remaining oxide to mixed carbide of iron and manganese occurs, and growth of the carbide phase covering the surface of the partially reduced ore particles is seen. The rate of reduction / metallization during this stage is substantially slower compared to Stage 1, and the extent of reduction / metallization does not improve much, reaching a maximum of 73% at 1200°C.

THE KINETICS OF REDUCTION

The present experimental data for manganese ore was analysed by using the following approach:

(1) When the overall rate is controlled by the chemical reaction at the interface, which is the principal resistance to the progress of reaction, then the rate equation can be expressed in terms of fraction reacted as follows:

$$kt = [1 - (1 - F)^{1/3}] \quad [4]$$

where:
F = fraction reacted
k = rate constant
t = time

(2) When the overall rate is controlled by diffusion through the product layer, the rate of reaction may be written in terms of fractional conversion as:

$$kt = \left[1 - 3(1 - F)^{\frac{2}{3}} + 2(1 - F)\right] \quad [5]$$

In this work, the initial rates that correspond to the first stage were evaluated as slopes of experimental metallization versus time curves, the logarithms of which were plotted with respect to inverse temperature, as shown in Figures 16 and 17. The activation energies obtained by this method, in the temperature range of 1050°C to 1250°C, varied from 1.4639 kJ/mol to 24.72 kJ/mol for manganese, and from 0.287 kJ/mol to 14.798 kJ/mol for Fe, which were too low for chemical reaction rate control, indicating potential gaseous diffusion control. The values are also much lower than the ones reported by Akdogan (1992) (for temperatures from 1100°C to 1350°C) as 81.3 kJ/mol to 94.6 kJ/mol for ordinary solid-state carbothermic reduction of Wessels manganese ores. In their study on pre-reduction of manganese ore for ferromanganese smelting, Mishra and Khangaoukar (1975) reported an apparent activation energy value of 38 kJ/mol and attributed this value to the gaseous diffusion rate-controlling mechanism.

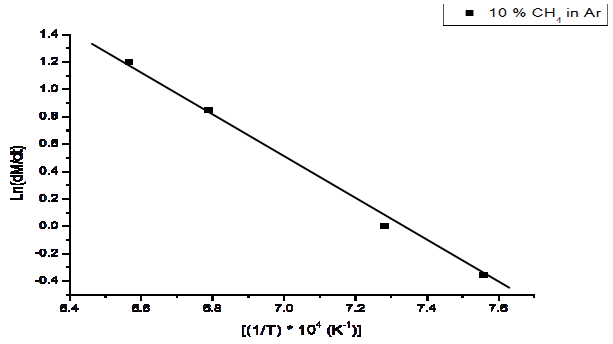

Figure 16: Determination of activation energy for Mn metallization with 10% Methane + Argon (E_A =13.3024 kJ/mol)

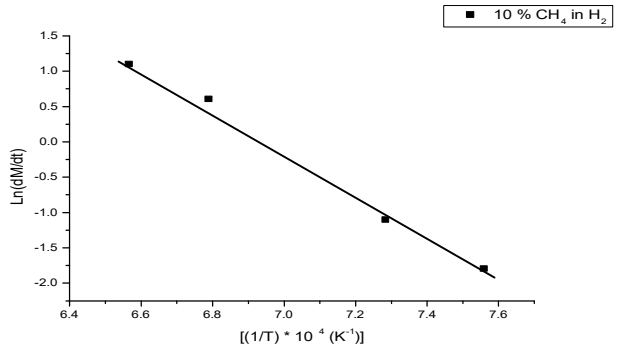

Figure 17: Determination of activation energy for Mn metallization with 10% Methane + Hydrogen (E_A = 24.72 kJ/mol)

Mathematical analysis

As the metallization of manganese oxide (MnO) of the ore proceeds carbothermically (see below) by the action of high-activity carbon particles continuously precipitating from the CH_4–H_2 or CH_4–Ar gas mixture and then continuing through CO gas reduction and regeneration of CO gas by the solid carbon particles, the mathematical analysis is done for a binary gas mixture of CO–CO_2 for which the diffusivity is independent of gas composition. Another reason for the adoption of this approach is the lack of data, especially for methane- and hydrogen-containing gases, thus the effect of the other gaseous species in the gas phase was neglected. However, the calculated values for the CO–CO_2 gas mixture from the experimental data are actually apparent values incorporating indirectly the effect of the other gases. Another consideration for the justification of this assumption is the fact that hydrogen in the gas phase, thermodynamically, cannot reduce MnO, for which this mathematical treatment applies. Furthermore, because of the relatively high thermal conductivity of the metal oxides, energy transfer can be dismissed as a possible rate-controlling process. With these justified implications, the mathematical formulation is based on the assumptions:

1. As the reaction, on the pore walls, of oxide is accompanied by gas diffusion, depending on the porosity and gas diffusivity therein, there will be partial internal metallization slightly ahead of a nominal product / oxide interface, resulting in a rather diffuse interface.
2. Quasi–stationary conditions prevail for a first-order type reaction involving CO and CO_2 in a spherical porous particle.
3. The resistance to the film diffusion around the particle is negligibly small.
4. Isothermal and isobaric conditions exist.

The mathematical development for this stage is very complex and involved, and is beyond the scope of this article. However, it is based on the principle given by Ishida and Wen (1968), and details can be found in their article.

At the end of the first stage, the fractional conversion is given by the following equation:

$$F_f = 3\,((\emptyset_f \coth \emptyset_f - 1)/\emptyset_f{}^2)) \qquad [6]$$

where:
$\emptyset_f$ is the kinetic–diffusion modulus, also known as the Thiele modulus. $\emptyset_f$ is used in the study of reactions on a catalyst to show the effect of gas diffusion on the reaction rates on catalyst pore walls, and is defined as

$$\emptyset_f = \left(\frac{kS\rho\left(\frac{(K_e+1)}{K_e}\right)}{D_{ef}}\right)^{\frac{1}{2}} . r_p \qquad [7]$$

where K_e is the equilibrium constant of the reduction reaction shown below.

$$Mn_3O_4 + CO = 3\,MnO + CO_2 \qquad [8]$$

D_{ef} is the effective diffusivity of (CO) and (CO_2); S is pore surface area; ρ is density of a particle; k is the rate constant; K_e is the equilibrium constant; and r_p is the initial radius of a particle. The values of effective CO–CO_2 diffusivities generated by the model were found to lie in the range from $1.45*10^{-6}$ cm^2s^{-1} to $8.427*10^{-6}$ cm^2s^{-1}, which are much lower than the intermolecular diffusivities calculated by using the theoretical equation based on the kinetic theory and Lennard-Jones expression for intermolecular forces. It can be deduced that, in the present study, Knudsen diffusivity is the predominant mode of diffusion, with molecular diffusion playing a very minor role. Diffusive flux occurs via two diffusional processes: molecular diffusion and Knudsen diffusion in porous media. In most of the cases previously reported by Pomfret and Grieveson (1978), Knudsen diffusivity values were several orders lower than those of molecular diffusivity. Because the effective diffusivity values generated by the model are so much lower than the molecular diffusivity values, it can safely be assumed that in this case Knudsen diffusion is the predominant mode of diffusion. The value of Knudsen diffusivity calculated for the present study is $2.7611*10^{-6}$ cm^2s^{-1} at 1100°C, which is in reasonable agreement (considering the temperature difference) with the value for Knudsen diffusivity calculated by Grimsley (1977) for the ordinary carbothermic reduction of Mamatwan manganese ore at 1300°C, which is $3.03*10^{-5}$ cm^2s^{-1}. Grimsley (1977) also calculated the effective CO–CO_2 diffusivities, which were in the range from $7.9*10^{-5}$ cm^2s^{-1} to $1.59*10^{-4}$ cm^2s^{-1}. He also attributed these values to the major role played by Knudsen diffusion.

The model prediction of the reduction percentage during the second stage of the reduction, F_s, can be found from the following equation used by King and Brown (1980) for impervious core reactions.

$$F_s = 1 + \delta^3{}_s\, F_f - \delta^3{}_s \qquad [9]$$

where F_s is the fractional conversion at the end of the second stage. δ_s, the dimensionless radius during the second stage of the reduction, is calculated by the following equation.

$$\delta_s = 1 - \frac{M_s}{3C_{SO}\, r_p}(t - t_f) \quad [10]$$

where M_s is the rate of metallization during the second stage; t_f is the time taken to complete the first stage; and, r = r_p ; C_{SO} = initial concentration of solid reactant. Equation [10] gives the position of the outer interface during the second stage at time (t). In order to determine δ_s, certain key parameters, such as the time to complete conversion ($t_{tot.}$) and the dimensionless time taken for complete conversion of MnO as a shrinking core (θ_r), had to be estimated by using the experimental data of the metallization during the second stage. The time required for the reaction to complete both the first stage and the second stage, t_{tot}, can be found from the following equation.

$$t_{tot} = t_f + (3C_{SO}\, r_p / M_s) \quad [11]$$

A dimensionless ratio of the time to complete the first stage to the time taken for complete metallization of MnO as a shrinking core can be defined as:

$$\theta_r = 3kS\rho C_g\, r_p / M_s \quad [12]$$

where C_g is total gas concentration. The time to complete conversion was estimated by using the experimental values. The t_f was taken as 30 minutes. The M_s value changed between 1.83*10^{-8} mol.s^{-1}.cm^{-2} and 8.55*10^{-8} mol.s^{-1}.cm^{-2}. Specific rate constant values for the second stage (k_s) vary from 5.5277*10^{-6} cm/s to 3.1581*10^{-5} cm/s, which are much smaller than the specific rate constant for the first stage of reduction (k_f), which varied from 1.64*10^{-4} cm/s to 1.146*10^{-4} cm/s, as the rate of the second stage of the reduction is much slower than the rate of the first stage. The value of M_s estimated was then used in equation [11] from which the time to complete conversion can be predicted. These values were later inserted in equation [12] and equation [10] to predict the parameters θ_r and δ_s , which were used to calculate the value of F_s.

The application of the model to the experimental data can be demonstrated by studying the nature of plots of Ms versus time. These plots are given below in Figures 18 to 21.

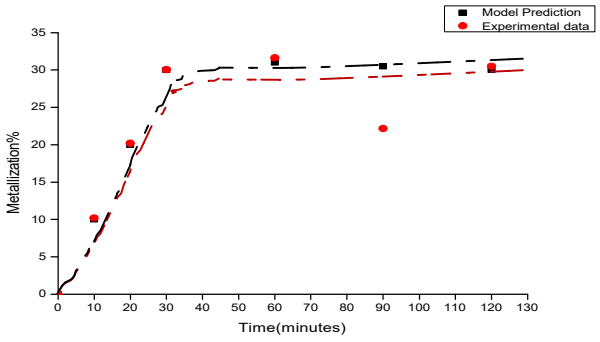

Figure 18: Model prediction compared with experimental data for 10% CH_4 in Ar at 1100°C

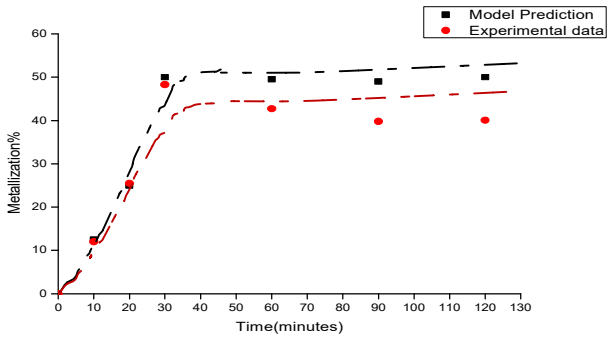

Figure 19: Model prediction compared with experimental data for 10% CH_4 in H_2 at 1100°C

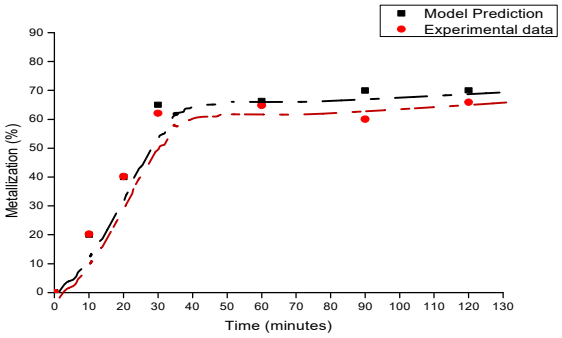

Figure 20: Model prediction compared with experimental data for 30% CH_4 in Ar at 1100°C

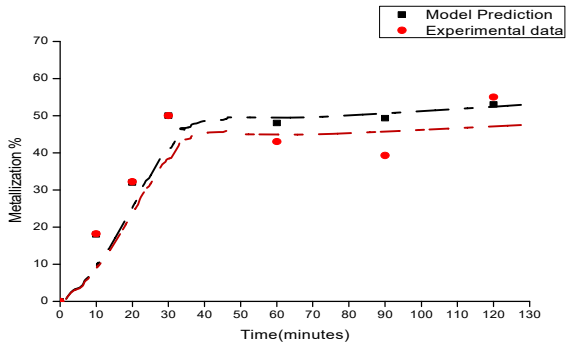

Figure 21. Model prediction compared with experimental data for 30% CH_4 in H_2 at 1100°C

Although the theoretically derived metallization curves fit the experimental curves reasonably well, there are deviations which may have a number of explanations. A major cause for the lack of complete agreement between theoretical and experimental results may lie in the complex mineralogy of the ore, as well as the rather complex gas mixture actually existing including not only CO and CO_2 but also hydrogen, methane, and argon. The model should, therefore, be regarded as a useful simplification for data analysis to describe the metallization mechanism of Mamatwan ore.

CONCLUSIONS

The reduction/metallization of Mamatwan manganese ore through the use of methane gas is principally a carbothermic reduction possibly assisted by hydrogen gas. The maximum 73% metallization was achieved in a methane/argon gas mixture at 1200°C in less than 2 hours. The extent of the reduction as well as the Mn/Fe ratios in the resulting alloy were higher than those in ordinary carbothermic solid-state reduction at these temperatures. The activation energy obtained by this method in the temperature range of 1050°C to 1250°C varied from 1.464 kJ/mol to 24.72 kJ/mol, indicating the possibility of diffusional control. The values of effective $CO–CO_2$ diffusivities generated by the model were found to lie in the range from $1.45*10^{-6}$ cm^2s^{-1} to $8.427*10^{-6}$ cm^2s^{-1}, which are much lower than the intermolecular diffusivities calculated by using the theoretical equation based on the kinetic theory and Lennard-Jones expression for intermolecular forces. The value of Knudsen diffusivity calculated for the present study is $2.7611*10^{-6}$ $cm^2.s^{-1}$ at 1100°C. The values of the rate of metallization during the second stage (Ms) changed between $1.83*10^{-8}$ $mol.s^{-1}.cm^{-2}$ and $8.55*10^{-8}$ $mol.s^{-1}.cm^{-2}$. The specific rate constant values for the second stage (k_s) varied from $5.528*10^{-6}$ cm/s to $3.158*10^{-5}$ cm/s, which are smaller than the specific rate constant for the first stage of reduction (k_f), which varied from $1.64*10^{-4}$ cm/s to $1.146*10^{-4}$ cm/s, as the rate of the second stage of the reduction is slower than the rate of the first stage. As shown in this work, solid-state pre-reduction of manganese ore by the use of methane can well be an alternative process route, as it produces highly metallized products (+ 70%) at relatively low temperatures around 1250°C with high Mn to Fe ratios. This can then be followed by a simple melting and separation process while finalizing the reduction possibly by the use of an open arc furnace rather than the submerged arc furnaces in use today. This combination has the potential to reduce energy consumption and carbon footprint.

ACKNOWLEDGEMENTS

The authors wish to thank South32 for partially supporting this research work.

REFERENCES

Akdogan G. 1992. Kinetics and mechanism of the solid state carbothermic reduction of Wessels type ferro manganese ores, PhD Thesis, University of the Witwatersrand, Johannesburg.

Anacleto N., Ostrovski O., and Ganguly S. 2004. Solid state reduction of manganese oxides by methane - containing gas, *ISIJ International*, 144, pp.1480–1487.

Burucu E. 1991. Kinetics and mechanism of the reduction of Mamatwan manganese ore fines by solid carbon, MSc Dissertation, University of the Witwatersrand, Johannesburg.

Grimsley W.D. 1977. A study of the characteristics and mechanism of reduction of manganese ore by solid carbon, MSc Dissertation, University of the Witwatersrand, Johannesburg.

Ishida M. and Wen C.Y. 1968. Comparison of kinetic and diffusional models for solid–gas reactions, *AICHE Journal*, Vol.14, No.2, pp.311–317.

King R.P. and Brown C.P. 1980. *Met. Trans*, Vol.11b, pp.585–592.

Kononov R., Ostrovski O., and Ganguly S. 2008. Carbothermal reduction of manganese oxide in different gas atmosphere, *Metallurgical and Materials Transactions B*, 39B, pp.662–668.

Mishra V.N. and Khangaoukar P.R. 1975. Pre-reduction of Indian manganese ores", *Jr. Instn of Engrs (India)*, Vol.55 mm, No.283, pp.59–63.

Ostrovski O., Anacleto N., and Ganguly S. 2004. Reduction of manganese ores by methane-containing gas, Infacon X: Proceedings of the Tenth International Ferroalloys Congress, Cape Town, South Africa, 1–4 February 2004, pp. 173–183.

Ostrovski O. and Zang G. 2006. Reduction and carburization of metal oxides by methane containing gas", *AICHE Journal*, 52, pp.300–310.

Pomfret R.J. and Grieveson P. 1978. Kinetics of fast initial stage reduction of MnO from silicate slags by carbon in molten iron, *Iron and Steelmaking*, No.5, pp.191–197.

Amit Bhalla

Researcher, University of the Witwatersrand

Amit has obtained his B.Tech from I.I.T. Kanpur and M.S., PhD (2017) from the University of the Witwatersrand. He has experience of working in the steel industry and foundry. His research interests are in the area of pyrometallurgy.